Advanced Review

Theoretical study of crystal phase effect in heterogeneous catalysis

Jin-Xun Liu[1,2†] and Wei-Xue Li[1,2*]

Density functional theory (DFT) is a powerful tool to study heterogeneous catalysis nowadays. In past decades, numerous DFT calculations have been conducted to investigate the mechanism of catalytic reaction from which the rationale of catalyst design can be revealed. Because the catalyst electronic and geometric structures determine the intrinsic activity, corresponding composition, size, and morphology have been explored extensively to tune the structure–activity relationship for higher activity and selectivity. In this review, we focus on the recent theoretical progress of the crystal phase effect on catalysis. Catalysts with different crystal phases have different symmetries, and could expose very different facets with distinct electronic and geometrical properties, which would have significant influential on the activity and selectivity of the active sites as well as the site density. Exploration of the dependence of catalysis on the crystal phases provides a new rationale of catalysts design toward a high-specific activity. © 2016 John Wiley & Sons, Ltd

How to cite this article:
WIREs Comput Mol Sci 2016, 6:571–583. doi: 10.1002/wcms.1267

INTRODUCTION

Designing the catalysts with higher activity, selectivity, and stability is the key topics of heterogeneous catalysis. Once the relationship between precise structure and intrinsic activity of the active sites (namely, structure sensitivity) is known, synthesis of the catalysts could be guided to expose more active sites for better activity and selectivity in experiment. However, under the realistic reaction conditions, industrial catalysts always consist of small nanoparticles with high surface area exhibiting lots of step edges, kinks, crystal facets, interface, etc. It is therefore difficult to clarify the structure sensitivity unambiguously because of the complexity of surface structures and non-uniformity of the realistic catalysts.[1] Identification of the structure sensitivity of catalysts in chemical reactions to achieve the maximum mass-specific yet stable reactivity, although is still a great challenge in heterogeneous catalysis, will assist in the rational design of new catalytic systems and accelerate the evolution of the field of nanotechnology.[2]

With the development of density functional theory (DFT) and the improvement of computational capabilities, surface properties of the catalytic materials and chemical reactions mechanism can be revealed at the atomic level. Microscopic understanding of chemical reactions on model-catalysts, identification of the structure sensitivity, as well as obtaining the important reaction intermediates by DFT calculations can guide to synthesize highly efficient and stable catalysts in experiment. It is well documented that the catalytic activity and selectivity are determined by the electronic and geometric structure of the catalysts.[3] Thus, designing efficient catalysts can be realized by changing the composition, morphology, particle size, and supports, formation of interface, addition of promoter, etc.[4–8]

Besides as the stated above effects, it is found that the catalytic activity and selectivity can be

†Current address: Department of Chemical Engineering at Eindhoven, University of Technology, The Netherlands

*Correspondence to: wxli70@ustc.edu.cn

[1]College of Chemistry and Material Sciences, iChEM (Collaborative Innovation Center of Chemistry for Energy Materials), CAS Center for Excellence in Nanoscience, University of Science and Technology of China, Hefei, China

[2]Hefei National Laboratory for Physical Sciences at the Microscale, Hefei, China

Conflict of interest: The authors have declared no conflicts of interest for this article.

 © 2016 John Wiley & Sons, Ltd

controlled further by the crystal phase of the catalysts.[9–17] The catalysts with different crystal phases have distinct atomic packing sequence and symmetries, which will expose very different surface structure and morphology with distinct activity, selectivity, and site population. Dependence of the different surface sites that may occur and their population on the crystal phases open a new dimension to the design of stable catalyst with high mass-specific activity. In this review, we have outlined recently progresses of the crystal phase effect on catalysis by DFT calculations. The rest of this paper can be divided into five parts: crystal phase effect of cobalt (Co) and ruthenium (Ru) metals, Co carbide versus Co metal, iron (Fe) carbide versus Fe metal, rutile versus anatase phase of titania (TiO_2) oxide, conclusions, and perspectives will be drawn finally.

CRYSTAL PHASE EFFECT OF COBALT AND RUTHENIUM METALS

Transition metals can crystallize for instance in either hexagonal close-packed (HCP) or face-centered cubic (FCC) or body-centered cubic (BCC) structures. Under the standard conditions, their bulk crystal structures change from HCP to BCC, HCP, FCC from left to right of the periodic table of element (Figure 1), mainly because of the different electronic configuration.[18] However, when the environment condition (temperature, pressure, and particle size) varies, the favorable crystal phase of the given transition metal could transform from one to another with different atomic stacking sequence and symmetry.[16,19–27] Here, we take Co and Ru as an example because of their wide application in heterogeneous catalysis. Co has an HCP crystal structure under ambient atmospheres. However, it is found that HCP Co could be transformed into FCC Co when the temperature increase up to 400°C.[26] In addition, Co crystal phase transformation (HCP → FCC) could occur with decreasing the particle size. When Co particle size is larger than 40 nm, HCP Co is the predominant phase with inclusion of a very small amount of FCC Co. Pure FCC Co could be found when the particle size decreases to 20 nm.[27] Ru in the bulk phase adopts an HCP structure at all temperature, while FCC Ru uniformly size nanoparticle was recently obtained at room temperature by using special precursor.[16]

Fischer–Tropsch synthesis (FTS) is an important process for producing liquid fuels and other chemicals via syngas (a mixture of carbon monoxide and hydrogen molecule) from coal, natural gas, shale gas, biomass, etc.[28,29] Co is the common used FTS catalyst which have attracted much more

Sc HCP	Ti HCP	V BCC	Cr BCC	Mn BCC	Fe BCC	Co HCP	Ni FCC	Cu FCC	Zn HCP
Y HCP	Zr HCP	Nb BCC	Mo BCC	Tc HCP	Ru HCP	Rh FCC	Pd FCC	Ag FCC	Cd HCP
La HCP	Hf HCP	Ta BCC	W BCC	Rc HCP	Os HCP	Ir FCC	Pt FCC	Au FCC	Hg ORTH

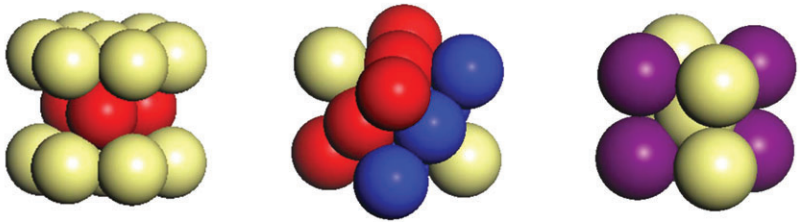

HCP (D_{3h}) FCC (O_h) BCC (O_h)

FIGURE 1 | The crystal structures (under standard conditions) of transition metal in the periodic table of element. The point groups are indicated for the three typical crystal structures.

 © 2016 John Wiley & Sons, Ltd

attention recent years because of its high activity for C_{5+} formation and relatively low cost.[30] Further improvement of CO conversion activity and selectivity for C_{5+} hydrocarbons on Co-based catalysts is still a long-standing issue. Over the past few years, numerous studies have been conducted to understand the nature of structure sensitivity of Co-based catalysts for FTS by well-defined preparation methods, *in situ* characterization technology, surface science studies, and *ab initio* DFT calculations. Two typical structure sensitivities have been observed for FTS over Co catalysts, i.e., crystal structure and particle size effect. It is found that Co crystalline phase transformation could occur by changing the catalyst size,[27] varying the supports and promoters, and pretreating the catalysts.[31–33] This crystal structure changes will play a significant role in the activity and selectivity for FTS catalysis. It has been reported by many group that HCP Co has higher FTS activity than FCC Co.[9,10,14,34–37] As proposed by Ducreux et al., the catalysts with majority of HCP phase has higher CO conversion activity under FTS conditions compared with those containing predominantly FCC phase particles.[9] FCC Co was the dominant phase in the Co-based catalysts reduced in hydrogen, whereas HCP Co could be produced by consecutive CO and hydrogen treatments. Another experimental work shows that HCP Co is more active than FCC phase, while Co_2C is inactive for FTS.[14] Davis and coworkers[37] have also presented similar results that Co containing HCP phase presenting higher CO conversion and less methane selectivity compared with the catalysts containing FCC phase under similar FTS reaction conditions.

However, it remains open as to whether and why HCP Co catalysts have higher activity and lower selectivity for methane than FCC Co, which prevents the full exploration of this structure sensitivity. To set light on the effect of the Co crystallographic structures (HCP and FCC Co), CO activation as a probe reaction has been investigated extensively through first principles DFT calculations, because this elementary step is crucial for the reaction mechanism and the overall reactivity of the FTS.[38] HCP and FCC Co have quite different bulk symmetries and atomic packing sequence, and these are essential for the type of the exposed facets with distinct surface topologies and their relative ratio (so-called morphology), which will be decisive for the intrinsic activity/selectivity of the individual facets exposed and the contribution to the overall reactivity. The morphologies of HCP and FCC Co can be approximately obtained via the Wulff construction (Figure 2) based on the calculated surface energies. It is found that HCP and FCC Co have different shapes stemming from their different symmetries. Bulk HCP Co belongs to the D_{3h} point group, and the corresponding morphology is a dihedral-like shape with two close-packed (0001) facets. The other open facets occupy almost 70% of the overall surface area. On the other hand, FCC Co belongs to the O_h point group with very high symmetry, and the corresponding morphology is an octahedron-like shape, where eight close-packed (111) facets are exposed, covering predominantly 80% of the total surface area.

Based on a simple micro-kinetic model and calculated CO activation barriers, CO dissociation reaction rate is calculated and shown in Figure 2. It can be found that there are at least four facets, namely, $(11\bar{2}1)$, $(10\bar{1}1)$, $(10\bar{1}2)$, and$(11\bar{2}0)$) on HCP Co, having reaction rates higher than that of the most active FCC (100) among all the FCC Co exposed facets. This is because all these four HCP facets have lower CO dissociation barriers. In fact, HCP Co has a number of distinct facets available with significantly higher reaction rates because of the presence of the more favorable active facets (B5 site) than the most active FCC (100) facet (Figure 3). This indicates that CO dissociation on both HCP Co and FCC Co is highly activated and quite structure sensitive. HCP Co has higher activity than FCC Co for CO activation. It would be highly valuable to synthesize HCP Co exposing the most active four facets for higher mass-specific reactivity.

For FTS, CO may also dissociate by hydrogen-assisted pathway,[39–42] which could change the above scenario based on the direct route. It is found that CO activation reaction pathway will be quite different on the two phases, i.e., the direct route for HCP Co and the H-assisted route for FCC Co. This could be rationalized by the higher activity of the HCP Co for the direct route leaving little room for the H-assisted route (Figure 4). Even considering the presence of hydrogen, HCP Co remains more active than FCC Co for CO activation.

Ru is another significant material in heterogeneous catalysis. Although Ru with FCC structure does not exist in the bulk Ru phase diagram, Kitagawa et al.[16,43] have synthesized FCC Ru nanoparticle at room temperature because of the nano size effect. From Figure 5, it is found that, above 3 nm, the newly discovered FCC Ru nanoparticles were more reactive than the conventional HCP Ru nanoparticles for CO oxidation. It has been proposed that the mechanism of CO oxidation with HCP Ru begins with the oxidation of (0001) surface in the formation of a few RuO_2 (110) layers, which is considered as the active phase for CO oxidation on Ru

 © 2016 John Wiley & Sons, Ltd

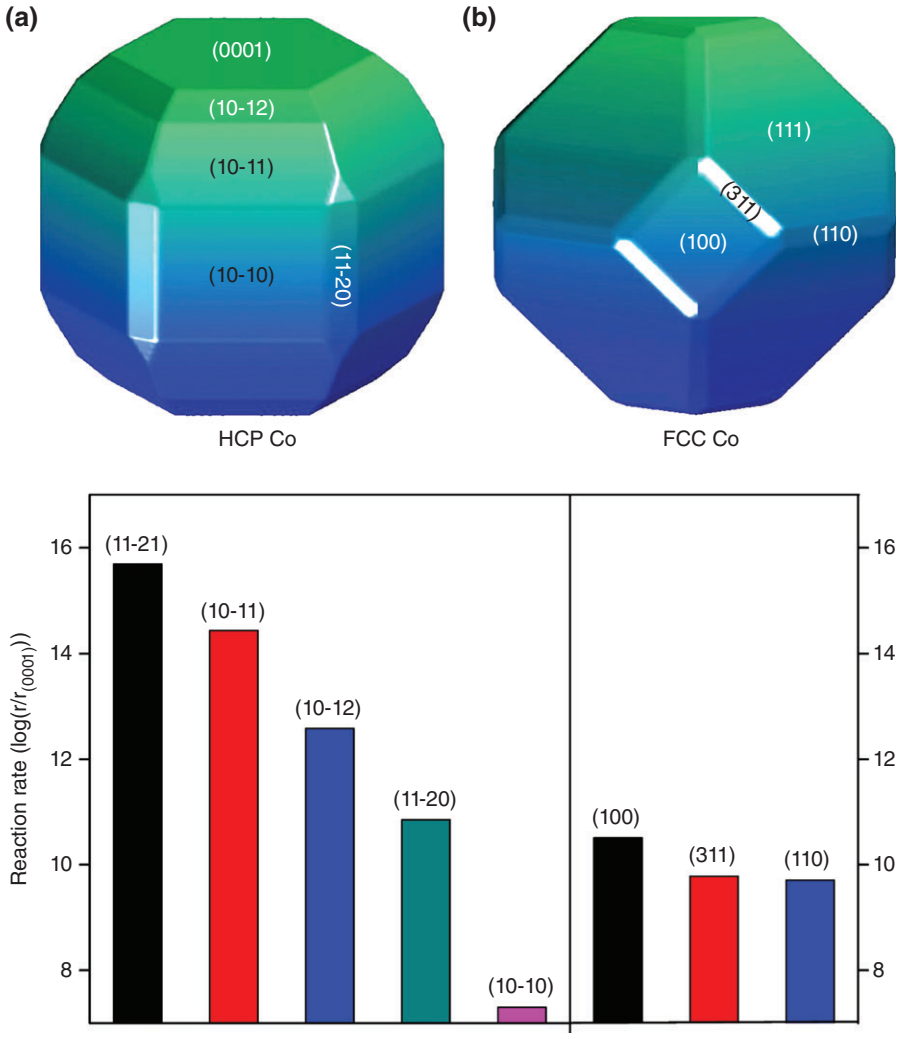

FIGURE 2 | Equilibrium morphology of HCP and FCC Co based on the Wulff construction and calculated reaction rates r for CO dissociation on exposed HCP and FCC Co facets at the low coverage. All rates are normalized by that of HCP (0001) with units of s^{-1} $site^{-1}$. (Reproduced with permission from Ref 38. Copyright 2013 American Chemical Society.)

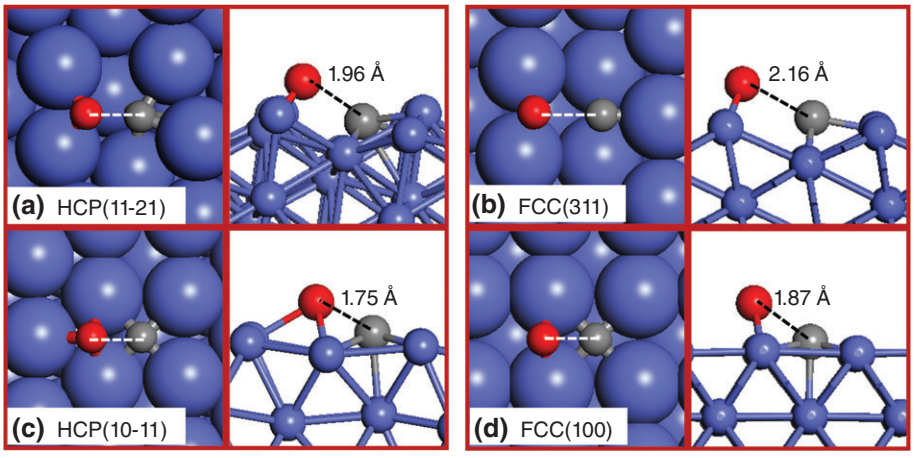

FIGURE 3 | Top and side view of optimized transition states for CO dissociation on FCC and HCP Co surfaces. Blue, red, and gray balls represent Co, O, and C atoms, respectively. (Reproduced with permission from Ref 38. Copyright 2013 American Chemical Society.)

 © 2016 John Wiley & Sons, Ltd

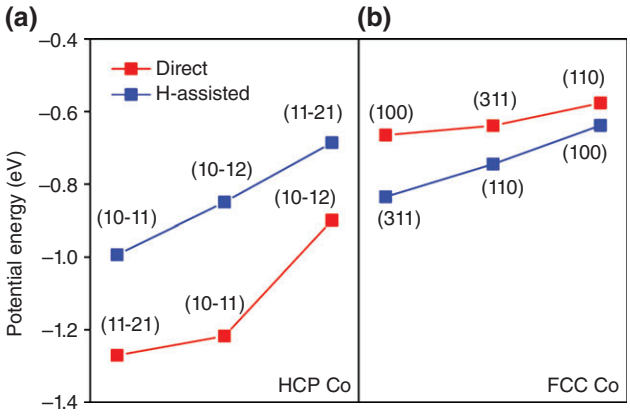

FIGURE 4 | Calculated potential energy (in eV) for CO activation at the transition states for breaking the C═O bond via the direct route (CO* + H* → C* + O* + H*) (red) and the H-assisted route (CO* + H* → CHO* → CH* + O*) (blue) on HCP and FCC Co surfaces. The zero energy reference is CO + $^1/_2$ H_2 in the gas phase. (Reproduced with permission from Ref 38. Copyright 2013 American Chemical Society.)

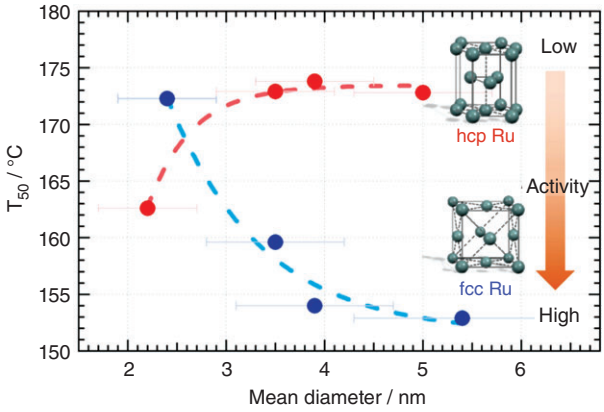

FIGURE 5 | Size dependence of the temperature for 50% conversion of CO to CO_2 (T_{50}) for FCC (blue) and HCP (red) Ru nanoparticles. (Reproduced with permission from Ref 43. Copyright 2015 WILEY-VCH Verlag GmbH & Co. KGaA, Weinheim.)

catalysts.[44,45] The FCC (111) and HCP (0001) facets have common closely packed structures. FCC Ru nanoparticles generally tend to be enclosed by (111) surfaces because this facet has the lowest surface energy.[46] However, HCP Ru nanoparticles are not completely enclosed because of the existence of other different surfaces. Therefore, the FCC Ru nanoparticles could expose more active sites for CO oxidation exhibiting higher activity.

A newly phase control strategy was also developed by Zhang et al.[47] to prepare FCC Ru nanocatalyst, in which Ru shells were epitaxially grown on the surfaces of FCC Pt and Pd seeds and the seeds guided the Ru shells inheriting the FCC structure. It is found that the synthesized Pt@Ru nanoparticles showed not only the pure FCC phase but also high morphology selectivity to tetrahedrons surrounded by {111} facets. DFT calculations indicate that the preferentially epitaxial growth of Ru atom layers on the nonclosest-packed facets of hetero FCC metal seeds lead to the formation of FCC Ru shells (Figure 6). The synthesized FCC Pt@Ru tetrahedrons/C exhibited greatly enhanced electro-catalytic activity toward hydrogen oxidation reaction (HOR) in acidic electrolyte compared with conventional hydrothermally synthesized HCP Ru catalysts. The optimum HOR activity should be achieved on well-crystallized FCC Ru catalysts exposing maximum {111} facets. In addition, Lee and coworkers[48] reported a novel, seed-dependent synthesis of FCC Ru which is also highly active for oxygen evolution reaction.

Above results show that the catalytic activity is strongly influenced by the crystal structures of transition metals. Moreover, it is dependent on the type of chemical reactions. The insights revealed is constructive for the design of better, stable Co and Ru catalysts with maximum mass-specific reactivity, in which *ab initio* calculation and material synthesis would play an essential role.

COBALT CARBIDE PHASE VERSUS COBALT METAL PHASE

Precious Rh is the major catalysts for alcohol formation selectively via syngas. For this reaction, Rh with modest reactivity to dissociate CO partially is essential. Namely, it can dissociate CO molecules to produce C atom, which is hydrogenated to CH_x followed by C–C coupling to form hydrocarbon. On the other hand, there remains considerable CO in molecular states for insertion toward hydrocarbon producing the desired alcohol. Because of the considerable economic benefits of oxygenates/alcohol production and limitation usage of expensive Rh, it is urgent to find cheap and active catalysts to directly produce alcohols with low selectivity of other by-product, like light alkanes or methanol. Again, CO partial dissociation is prerequisite. Here, we will introduce a successful example for designing the Co metal/carbide interface, which is highly selective for high alcohol formation. Establishing the interface by using distinct catalytic properties of Co metal phase and its carbide phase is a new strategy for catalysts design.

The high alcohol synthesis is a significant process in basic chemical industries. This process is

 © 2016 John Wiley & Sons, Ltd

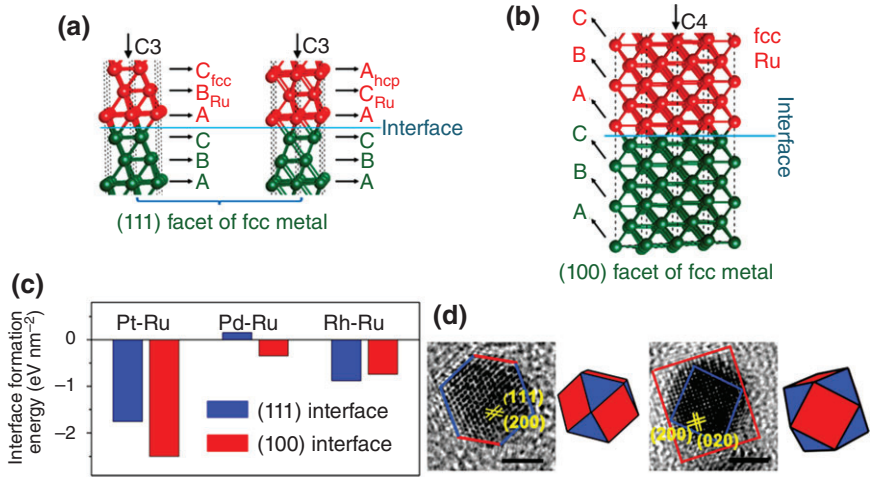

FIGURE 6 | Analysis of the interface between Ru and FCC noble metals. (a) and (b) are the formation of the interfaces between the Ru and other transition metals with FCC structure. (c) DFT calculated formation energies of (111) and (100) interfaces between FCC Pt, Pd, Rh, and Ru. (d) HRTEM images and 3D models of FCC Pt seeds with cubooctahedral morphology from (left) [01$\bar{1}$] and (right) [001] zone axes. Red and blue surfaces in these models represent {100} and {111} facets, respectively. The scale bars indicate 2 nm. (Reproduced with permission from Ref 47. Copyright 2015 American Chemical Society.)

involved in hydrogenation, ethylation, chain growth, oxidation, and hydrolysis.[49] It is found that metallic Co is only the active phase for FTS in the formation of long-chain hydrocarbons, while Co_2C has no activity and its formation considered as the sign of deactivation of the catalysts for FTS.[14] However, Ding et al. reported a one-step synthesis of aliphatic C_1-C_{18} α-alcohols high-quality fuels and low methanol from syngas via FTS process using nonprecious Co catalysts supported on an activated carbon.[50,51] Co carbide was observed after FTS reaction which may play a significant role in higher alcohol synthesis prosed by Mausbeck et al.,[52] Zaikovskii and coworkers,[53] and later by Wang et al.[54] The formation of Co_2C may be the origin for direct synthesis of high alcohols. From careful systematic experiment comparison, it is proposed that the formation of Co and Co_2C is the key for alcohol formation. DFT calculations also have been performed to clarify the active site and reaction mechanism for high alcohols formation on Co-based catalyst.[55]

Metal carbides are noble-metal-like and usually less active than the corresponding transition metal.[56,57] CO could non-dissociative adsorb on Co_2C which could provide adsorbed CO. In order to shed light on this, CO adsorption and dissociation are systematically studied on Co and Co_2C. From calculated density of states (DOS) (Figure 7), it can be found that Co_2C is metallic in nature, which is same with Co metal phase. Meanwhile, Co is a cation with a Bader charge of 0.48 e, and C is anion with Bader charge of about −0.99 e. The presence of Co–C coordination in first nearest neighbor of Co carbide is another difference with that of the Co metal phase with only Co–Co coordination. These lead to a great difference in their catalytic activity, as seen below.

Here, Co_2C (111) and Co (100) surfaces are considered to model Co_2C and Co catalysts,

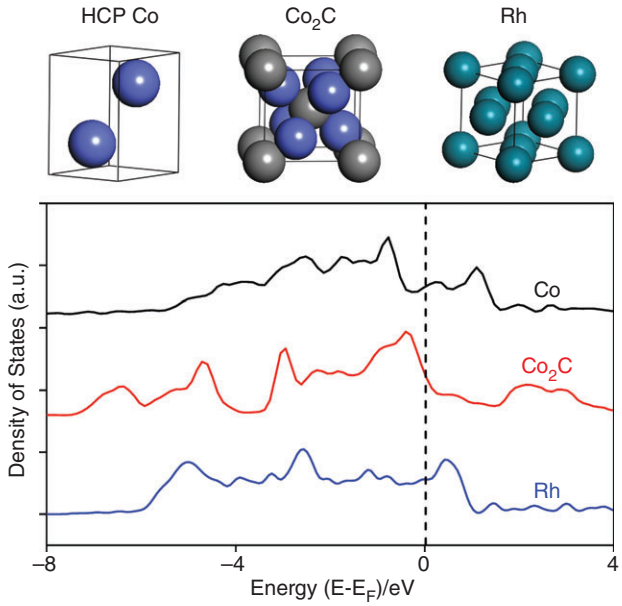

FIGURE 7 | The crystal structures and the corresponding density of state of bulk Co, Co_2C, and Rh.

 © 2016 John Wiley & Sons, Ltd

respectively. CO adsorbs much stronger on Co_2C (111) compared with that on Co (100) surface by 0.5 eV. The origin for this can be ascribed to the lattice expansion and positive charge of Co in Co_2C. The positive charge of Co could increase σ-donation from CO* greatly, which will enhance CO adsorption strength. However, the highly electronegative species, such as atomic C and O, is energetically unfavorable for binding the positive-charged Co in Co_2C. This can be ascribed as that the limited charge transfer from Co cation to C* and O* and their electrostatic repulsion with lattice C in Co_2C as well which would destabilize the overall energetics.

Stabilizing CO adsorption but destabilizing C* species on Co_2C will have a significant influence on the energetics and kinetics for CO dissociation. The calculated CO dissociation (CO* → C* + O*) reaction energy is thermal neutral (0.01 eV), while it is highly exothermic on Co (100) with the value of −0.75 eV. On Co_2C(111) surface, the calculated CO activation barrier is 2.18 eV, which is 0.69 eV higher than that on Co (111) surface. From Figure 8, it is found that CO dissociation has similar transition states on both surfaces and the dramatically decrease of reaction energy on Co_2C will suppress the corresponding kinetics. Under FTS reaction conditions, CO activation may be assisted by hydrogen, especially for the catalysts with relative low activity. The overall barrier is 2.12 eV for H-assisted CO activation pathway (CO* + H* → HCO* → CH* + O*) on Co_2C. While on Co (100), the total barrier for H-assisted pathway is 1.52 eV. Under FTS reaction conditions (493 K), CO cannot be activated efficiently on Co_2C (111) surface because of the significant high barrier. FTS chemical reaction cycle cannot be completed on Co_2C (111) because of the difficulty of CO activation under low temperature. Therefore, Co_2C (111), behaving as noble-metal-like, could provide efficient sites for non-dissociative adsorption of CO molecules.

Metallic Co is highly active and Co_2C is inert for FTS. When Co and Co_2C combine together, high alcohols will be produced. It indicates that dual-site at Co and Co_2C interface may be the active for CO activation. A simplified model is constructed, with a Co strip on Co_2C (111) surface. It is found that adsorbed CO on Co_2C can easily insert into the produced CH_2 intermediate on the Co strip with a low barrier of 0.77 eV. This modest value suggests that the interface is indeed facile for alcohol formation. However, CO insertion barrier is 1.48 eV on Co_2C (111) which is less active than the interface site. This illustrate that even hydrocarbon formed on Co metal might migrate to Co carbide, and the overall contribution to the alcohol formation would be quite lower, compared with the dual-sites at the Co and Co_2C interface (Figure 9). In addition, it is found that the interface between Co and Co_2C plays a significant role in ethylene hydroformylation. DFT calculations showed that the metallic Co sites can be used

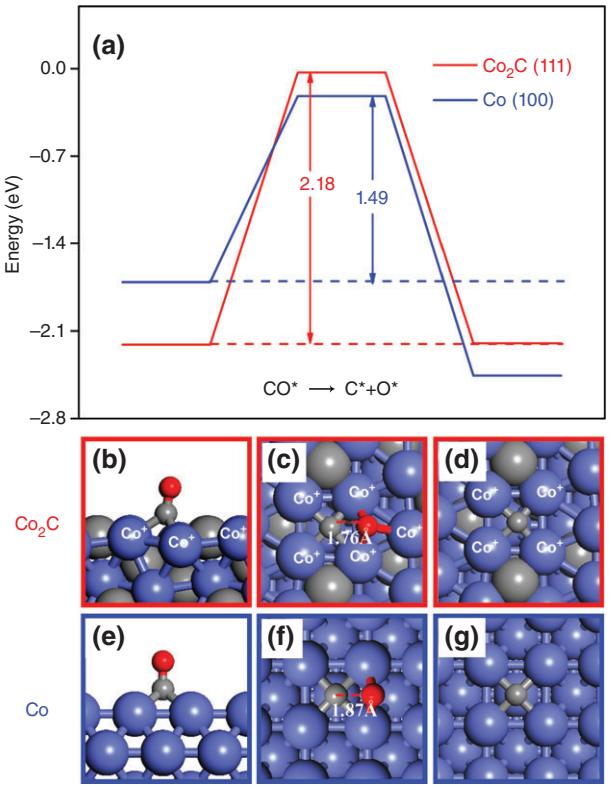

FIGURE 8 | Energetic and geometric information for direct CO activation on Co_2C (111) (red) and Co (100) (blue) surfaces. The corresponding CO adsorption, transition state, and C adsorption geometries are shown in (b)–(e). (Reproduced with permission from Ref 55. Copyright 2015 American Chemical Society.)

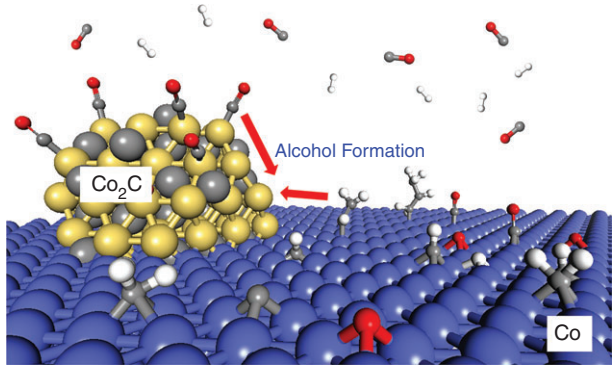

FIGURE 9 | Scheme for the high alcohol formation at interface between Co and Co_2C. (Reproduced with permission from Ref 55. Copyright 2015 American Chemical Society.)

© 2016 John Wiley & Sons, Ltd

for olefin adsorption and activation to form surface carbonaceous species, while Co_2C sites, for CO molecular adsorption, activation, and insertion for ethylene hydroformylation.[58] The interface between metal and its carbide phase, by using no-precious metal, provide the efficient dual active sites for oxygenates synthesis in syngas applications.

IRON CARBIDE PHASE VERSUS IRON METAL PHASE

Fe is the most widely used catalysts in FTS reaction and Fe-based catalysts have gained much attention owing to its low costs, a tunable product distribution, catalyzing the water-gas shift (WGS) reactions and effectively increasing H_2/CO ratio during FTS.[59] Under FTS reaction conditions, Fe-based catalysts are often a mixture of α-Fe, Fe_2C, Fe_3C, Fe_5C_2 and Fe_7C_3 etc. One of these phases could transform into another when the carbon potential changes. The identification of the active phase has long been controversial because of the prevention by complicated composition and *in situ* characterization of the catalysts. For example, metallic Fe,[60,61] $Fe_{2.2}C$,[62–65] Fe_7C_3,[66] Fe_5C_2 [59,67–70] had all been claimed as the active phase responsible for FTS. It remains an open question which is the active phase for FTS, i.e., Fe or Fe carbides. Fe and Fe carbides phases have very different electronic and geometries which will lead to distinct catalytic behaviors (adsorption mode, reaction mechanism, reactivity, and selectivity). Clarifying these issues will set up a direction for optimizing efficient Fe-based FTS catalysts. In order to uncover this important issue, DFT calculations have been conducted to study which is the active phase for FTS: Fe or Fe carbides.

The significant steps involved in FTS, including CO activation, methane formation, and C–C coupling, on Fe metal and carbide were investigated.[71] Stepped Fe-terminated Fe_5C_2 (100) and Fe (310) surfaces[72] having similar B5 sites were applied to model the two catalytic systems. These two surfaces were chosen because they are abundant and the exposed surface Fe atoms share similar local structure.[7,73,74] It is found that C atom adsorbs much stronger on Fe compared with that on Fe_5C_2 by almost 1 eV. From Figure 10(a), we can see that CO activation is feasible on Fe (310) and Fe_5C_2 (100) surfaces with low activation barriers (0.93 eV vs 1.38 eV). On Fe, CO dissociation barrier is lower than that on Fe_5C_2 (100) surface by about 0.4 eV stemming from the stronger adsorption of C atom. However, Fe_5C_2 is more active than Fe for C_2 and CH_4 formation with lower apparent activation

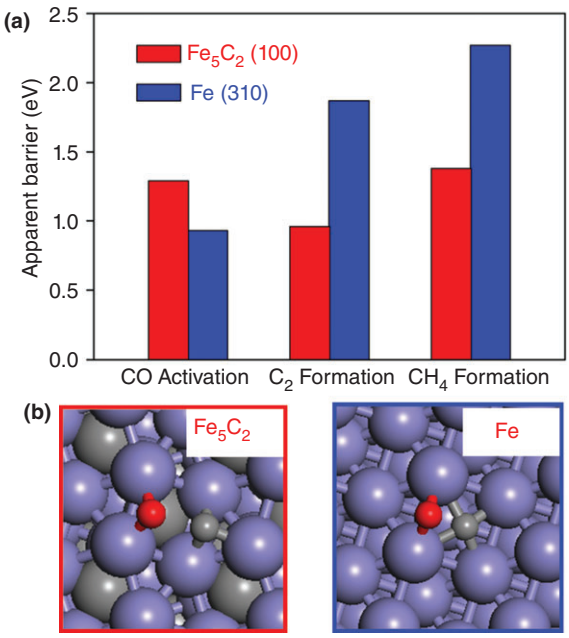

FIGURE 10 | (a) Apparent barriers for CO activation, C_2 and CH_4 formation on Fe_5C_2 (100) and Fe (310) surfaces. (b) The transition states for CO activation on Fe_5C_2 (100) and Fe (310) surfaces.[71]

barriers. C_2 and CH_4 formation are quite difficult on Fe under low temperature FTS conditions because of the high activation barriers of 1.87 and 2.27 eV, respectively. This can be ascribed to the too strong binding of the dissociated atomic carbon with surface Fe atoms which prevents the subsequent C–C coupling and methanation. While, for Fe_5C_2, the effective barriers for C–C coupling on Fe carbide were even lower than that of CO activation and methanation. This suggests once CO dissociates on Fe_5C_2, C–C bond formation would take place immediately. C–C bond will forms more easily on Fe carbide which are highly active for FTS with good olefin selectivity than that on Fe.

To support DFT calculations, pure phase metal and carbide catalysts, including α-Fe, Fe_5C_2, Fe_7C_3, and Fe_2C, have been synthesized and their FTS performance has been studied experimentally (Figure 11).[71] It is found that Fe_5C_2 is more active than pure Fe catalyst for FTS at the initial reaction period. From high-pressure stepwise temperature programming surface reaction (STPSR) experiment over Fe_5C_2 at 150°C, it is found that once CO were activated, C_2 (acetylene and ethylene) were observed simultaneously with water. Moreover, the larger apparent barrier of methanation (1.38 eV) than that of CO activation and C_2 formation implies that higher temperature for methane formation might be required. Indeed, STPSR experiment observed

 © 2016 John Wiley & Sons, Ltd

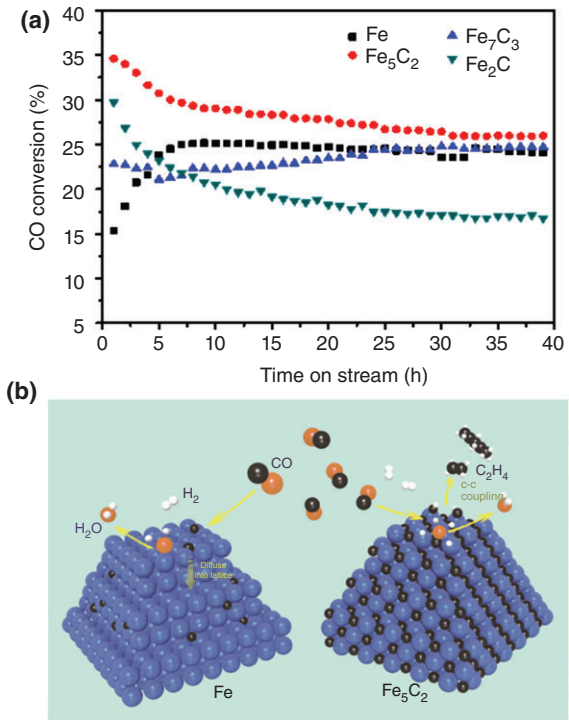

FIGURE 11 | CO conversion versus time over Fe, Fe_2C, Fe_7C_3, and Fe_5C_2 catalysts (reaction condition: 270°C, 30 bar, 20 ml/min syngas) (a); the scheme for CO hydrogenation on Fe and Fe_5C_2 (b).[71]

methane formation only when the reaction temperature reaching 190°C. While, for pure Fe catalyst, C_2 and methane will be generated when the temperature is higher than 170 and 190°C, respectively. This is because that CO dissociates easily on Fe, the dissociated carbon C* left on Fe surface could not be consumed by either the methanation or the C–C coupling because of their large effective barriers (2.27 and 1.87 eV). Indeed, there were no methane and C_2 hydrocarbon observed for 2 h at 150°C in STPSR experiment. The formed carbon would accumulate on the Fe surface, in the formation of Fe carbides which will be more active for C_2 and methane formation. Under FTS reaction condition (T = 150°C, P_{tot} = 2 MPa, H_2:CO = 2, $P(H_2O)$ = 0.01 MPa), the calculated ΔG for the formation of Fe_5C_2 [2CO (g) + 2H_2 (g) + 5 α-Fe (bulk) → Fe_5C_2 (bulk) + 2H_2O (g)] is −3.22 eV/Fe_5C_2. The large exothermic ΔG tells that the phase transition from the Fe to Fe_5C_2 is significantly favorable, which is nicely agreed with the experimental observation.[71] The insights revealed for the distinct activity of the different Fe phase, metal versus carbide, as well as the structural evolution under reaction condition are valuable for rationale design for Fe-based FTS catalysts.

RUTILE PHASE VERSUS ANATASE PHASE OF TiO_2

Transition metal oxide is another important catalytic material, and its crystal phase effect on catalysis has also been studied extensively. For instance, MnO_2 nanoparticles with different crystal phase can be synthesized using various approaches, and CO oxidation reactivity sequence is α- ≈ δ- > γ- > β-MnO_2.[75] Moreover, it is found that γ-Fe_2O_3 is more active than α-Fe_2O_3 for selective reduction of nitrogen oxide by ammonia.[17] For tuning the selectivity aspect, ZrO_2 with surface tetragonal crystal phase exhibits a high activity to form ethanol, while the ZrO_2 with surface monoclinic crystal phase presents a high activity to form isobutanol.[76]

TiO_2 is one of the promising catalysts for water splitting among various photoactive materials. Since the discovery of photocatalytic water splitting on TiO_2, identification of the active phase and active sites of TiO_2 has attracted much more attention in recent years. TiO_2 typically has two crystal phases: rutile and anatase. Bulk anatase is more stable compare with rutile under atmospheres conditions.[77] However, under low temperature or in small particle size conditions, rutile is thermodynamic more stable.[77,78] Many works showed that the crystalline phase of TiO_2 plays a significant role in photocatalysis and anatase is more active than rutile,[78,79] while rutile is often believed to be more active for oxidation reaction compared with anatase. Nevertheless, recent work showed that the presence of anatase would enhance the activity or even dominate the oxidation reaction.[80–82] Where is the active site located and how the titania crystal phase influences on the photo-activity are still elusive. In order to clarify which TiO_2 phase is the active phase for water splitting, DFT calculations have been performed on two common surfaces of two typical TiO_2 phases, i.e., anatase (101) and rutile (110).[83]

Based on the DFT calculations, it is found that first proton removal of water (H_2O + hole + → OH + H+) is sensitive to the TiO_2 crystalline phases and surfaces. The calculated barrier for O–H bond scission on rutile (110) surface is lower than that on anatase (101) by 0.2 eV. Rutile (110) surface is thus more active than anatase (101) surface for water splitting. The higher activity of rutile can be ascribed to the more favourable local bonding geometry of the surface. It is found that H_2O molecule could dissociate with a more favourable geometry on rutile, in which the transition state for water splitting has a better contact with both the Ti_{5c} and O_{2c} stabilizing the transition state. Zhao and Liu suggested that the surface structure sensitivity of

 © 2016 John Wiley & Sons, Ltd

water oxidation can be correlated to the geometrical separation between the exposed Ti_{5c} cation and its nearest O_{2c} anion, $d_{Ti_{5c}\text{-}O_{2c}}$, on the TiO_2 surface.[83] The DFT calculations showed that chemical properties of the surface play a significant role in the photocatalytic process, which is important for the design of new photocatalysts.

CONCLUSION

Catalytic activity and selectivity are closely related with the electronic and geometric structures of the active site of the catalysts. Besides particle size, morphology and interface effect, crystal phase of the catalysts have a great influence on catalysis. In this review, we have addressed the recent theoretical progress on crystal phase effects on catalysis, including transition metals Co and Ru for FTS, Co carbide and metal interface for alcohol synthesis, Fe carbide versus Fe metal phase for FTS, TiO_2 crystal phase effect on water splitting. These investigations provide not only a deep insight into the active sites and the structure sensitivity, but also the theoretical support for optimizing/designing the efficient and stable catalysts.

Because the catalysts with different crystal phases could exhibit distinct catalytic behavior, we could tune catalytic activity and selectivity by changing the corresponding crystal phases. There are lots of catalytic active transition metals in the periodic table of elements. Moreover, the favorable crystal phase including metal alloys could transform into different (even metastable) phase by changing reaction conditions (temperature and pressure), particle size, support, and pretreatment of the catalysts. Finally, under different reaction environments, transition metal could present in the form of oxide, carbides, sulfide, nitride, phosphide phase, etc. which will present dramatically different catalytic reactivity. The catalysts with different crystal phases combining together in the formation of interesting interface may also have an important influence on catalysis. Therefore, there is a large room to optimize the catalytic activity and selectivity by tuning the crystal phases. More investigations need to be carried out to find the most active phase with abundant active sites which are of great significance for catalysts design.

ACKNOWLEDGMENTS

This work received financial support from the National Basic Research Program of China (2013CB834603), the National Natural Science Foundation of China (21321002, 21225315), Chinese Academy of Sciences (XDA09030101). We thank Dr. Haiyan Su, Dr. Yunjie Ding, and Dr. Ding Ma for the fruitful discussions.

REFERENCES

1. Choudary BM, Mulukutla RS, Klabunde KJ. Benzylation of aromatic compounds with different crystallites of MgO. *J Am Chem Soc* 2003, 125:2020–2021.
2. Van Santen RA. Complementary structure sensitive and insensitive catalytic relationships. *Acc Chem Res* 2009, 42:57–66.
3. Norskov JK, Bligaard T, Rossmeisl J, Christensen CH. Towards the computational design of solid catalysts. *Nat Chem* 2009, 1:37–46.
4. Zhou K, Li Y. Catalysis based on nanocrystals with well-defined facets. *Angew Chem Int Ed* 2012, 51:602–613.
5. Den Breejen J, Radstake P, Bezemer G, Bitter J, Froseth V, Holmen A, Jong KP. On the origin of the cobalt particle size effects in Fischer–Tropsch catalysis. *J Am Chem Soc* 2009, 131:7197.
6. Fu Q, Li WX, Yao Y, Liu H, Su HY, Ma D, Gu XK, Chen L, Wang Z, Zhang H, et al. Interface-confined ferrous centers for catalytic oxidation. *Science* 2010, 328:1141–1144.
7. Huo C-F, Wu B-S, Gao P, Yang Y, Li Y-W, Jiao H. The mechanism of potassium promoter: enhancing the stability of active surfaces. *Angew Chem Int Ed* 2011, 50:7403–7406.
8. Jacobs G, Das TK, Zhang Y, Li J, Racoillet G, Davis BH. Fischer–Tropsch synthesis: support, loading, and promoter effects on the reducibility of cobalt catalysts. *Appl Catal Gen* 2002, 233:263–281.
9. Ducreux O, Rebours B, Lynch J, Roy-Auberger M, Bazin D. Microstructure of supported cobalt Fischer-Tropsch catalysts. *Oil Gas Sci Technol – Rev l'IFP* 2008, 64:49–62.
10. Ducreux O, Lynch J, Rebours B, Roy M, Chaumette P. *In-situ* characterisation of cobalt based fischer-tropsch catalysts: a new approach to the active phase. *Stud Surf Sci Catal* 1998, 119:125–130.

 © 2016 John Wiley & Sons, Ltd

11. Bezemer GL, Bitter JH, Kuipers HP, Oosterbeek H, Holewijn JE, Xu X, Kapteijn F, van Dillen AJ, de Jong KP. Cobalt particle size effects in the Fischer-Tropsch reaction studied with carbon nanofiber supported catalysts. *J Am Chem Soc* 2006, 128:3956–3964.
12. de la Peña O' Shea VA, de la Piscina PR, Homs N, Aromí G, Fierro JLG. Development of hexagonal closed-packed cobalt nanoparticles stable at high temperature. *Chem Mater* 2009, 21:5637–5643.
13. Khodakov AY. Fischer-Tropsch synthesis: relations between structure of cobalt catalysts and their catalytic performance. *Catal Today* 2009, 144:251–257.
14. Sadeqzadeh M, Karaca H, Safonova O, Fongarland P, Chambrey S, Roussel P, Griboval-Constant A, Lacroix M, Curulla-Ferré D, Luck F. Identification of the active species in the working alumina-supported cobalt catalyst under various conditions of Fischer–Tropsch synthesis. *Catal Today* 2011, 164:62–67.
15. Zhang Q, Deng W, Wang Y. Recent advances in understanding the key catalyst factors for Fischer-Tropsch synthesis. *J Energy Chem* 2013, 22:27–38.
16. Kusada K, Kobayashi H, Yamamoto T, Matsumura S, Sumi N, Sato K, Nagaoka K, Kubota Y, Kitagawa H. Discovery of face-centered-cubic ruthenium nanoparticles: facile size-controlled synthesis using the chemical reduction method. *J Am Chem Soc* 2013, 135:5493–5496.
17. Mou X, Zhang B, Li Y, Yao L, Wei X, Su DS, Shen W. Rod-shaped Fe_2O_3 as an efficient catalyst for the selective reduction of nitrogen oxide by ammonia. *Angew Chem Int Ed* 2012, 51:2989–2993.
18. Pettifor D. A physicist's view of the energetics of transition metals. *Calphad* 1977, 1:305–324.
19. Saunders N, Miodownik A, Dinsdale A. Metastable lattice stabilities for the elements. *Calphad* 1988, 12:351–374.
20. Xia H, Duclos SJ, Ruoff AL, Vohra YK. New high-pressure phase transition in zirconium metal. *Phys Rev Lett* 1990, 64:204.
21. Hasegawa H, Pettifor D. Microscopic theory of the temperature-pressure phase diagram of iron. *Phys Rev Lett* 1983, 50:130.
22. Yoo C-S, Cynn H, Söderlind P. Phase diagram of uranium at high pressures and temperatures. *Phys Rev B* 1998, 57:10359.
23. Shimizu K, Ishikawa H, Takao D, Yagi T, Amaya K. Superconductivity in compressed lithium at 20 K. *Nature* 2002, 419:597–599.
24. Errandonea D, Somayazulu M, Häusermann D, Mao H. Melting of tantalum at high pressure determined by angle dispersive X-ray diffraction in a double-sided laser-heated diamond-anvil cell. *J Phys Condens Matter* 2003, 15:7635.
25. Hrubiak R, Drozd V, Karbasi A, Saxena SK. High PT phase transitions and PVT equation of state of hafnium. *J Appl Phys* 2012, 111:112612–112616.
26. Hansen M, Anderko K, Salzberg H. Constitution of binary alloys. *J Electrochem Soc* 1958, 105: 260C–261C.
27. Kitakami O, Sato H, Shimada Y, Sato F, Tanaka M. Size effect on the crystal phase of cobalt fine particles. *Phys Rev B* 1997, 56:13849.
28. Schulz H. Short history and present trends of Fischer–Tropsch synthesis. *Appl Catal Gen* 1999, 186:3–12.
29. Baliban RC, Elia JA, Weekman V, Floudas CA. Process synthesis of hybrid coal, biomass, and natural gas to liquids via Fischer–Tropsch synthesis, ZSM-5 catalytic conversion, methanol synthesis, methanol-to-gasoline, and methanol-to-olefins/distillate technologies. *Comput Chem Eng* 2012, 47:29–56.
30. Tavasoli A, Abbaslou RMM, Trepanier M, Dalai AK. Fischer–Tropsch synthesis over cobalt catalyst supported on carbon nanotubes in a slurry reactor. *Appl Catal Gen* 2008, 345:134–142.
31. Fischer N, van Steen E, Claeys M. Preparation of supported nano-sized cobalt oxide and fcc cobalt crystallites. *Catal Today* 2011, 171:174–179.
32. Braconnier L, Landrivon E, Clémençon I, Legens C, Diehl F, Schuurman Y. How does activation affect the cobalt crystallographic structure? An in situ XRD and magnetic study. *Catal Today* 2013, 215:18–23.
33. Prieto G, Concepción P, Murciano R, Martínez A. The impact of pre-reduction thermal history on the metal surface topology and site-catalytic activity of Co/SiO_2 Fischer–Tropsch catalysts. *J Catal* 2013, 302:37–48.
34. Enache DI, Rebours B, Roy-Auberger M, Revel R. In situ XRD study of the influence of thermal treatment on the characteristics and the catalytic properties of cobalt-based Fischer–Tropsch catalysts. *J Catal* 2002, 205:346–353.
35. de la Peña O'Shea VA, Homs N, Fierro JLG, Ramírez de la Piscina P. Structural changes and activation treatment in a Co/SiO_2 catalyst for Fischer–Tropsch synthesis. *Catal Today* 2006, 114:422–427.
36. Karaca H, Safonova OV, Chambrey S, Fongarland P, Roussel P, Griboval-Constant A, Lacroix M, Khodakov AY. Structure and catalytic performance of Pt-promoted alumina-supported cobalt catalysts under realistic conditions of Fischer–Tropsch synthesis. *J Catal* 2011, 277:14–26.
37. Gnanamani MK, Jacobs G, Shafer WD, Davis BH. Fischer–Tropsch synthesis: activity of metallic phases of cobalt supported on silica. *Catal Today* 2013, 215:13–17.
38. Liu J-X, Su H-Y, Sun D-P, Zhang B-Y, Li W-X. Crystallographic dependence of CO activation on cobalt catalysts: HCP versus FCC. *J Am Chem Soc* 2013, 135:16284–16287.

 © 2016 John Wiley & Sons, Ltd

39. Huo C-F, Li Y-W, Wang J, Jiao H. Formation of CHx species from CO dissociation on double-stepped Co(0001): exploring Fischer–Tropsch mechanism. *J Phys Chem C* 2008, 112:14108–14116.
40. Inderwildi OR, Jenkins SJ, King DA. Fischer-Tropsch mechanism revisited: alternative pathways for the production of higher hydrocarbons from synthesis gas. *J Phys Chem C* 2008, 112:1305–1307.
41. Shetty S, Jansen APJ, van Santen RA. Direct versus hydrogen-assisted CO dissociation. *J Am Chem Soc* 2009, 131:12874–12875.
42. Ojeda M, Nabar R, Nilekar AU, Ishikawa A, Mavrikakis M, Iglesia E. CO activation pathways and the mechanism of Fischer-Tropsch synthesis. *J Catal* 2010, 272:287–297.
43. Kusada K, Kitagawa H. A route for phase control in metal nanoparticles: a potential strategy to create advanced materials. *Adv Mater* 2016, 28:1129–1142.
44. Over H, Kim Y, Seitsonen A, Wendt S, Lundgren E, Schmid M, Varga P, Morgante A, Ertl G. Atomic-scale structure and catalytic reactivity of the RuO_2 (110) surface. *Science* 2000, 287:1474–1476.
45. Gong X-Q, Liu Z-P, Raval R, Hu P. A systematic study of CO oxidation on metals and metal oxides: density functional theory calculations. *J Am Chem Soc* 2004, 126:8–9.
46. Teranishi T, Kurita R, Miyake M. Shape control of Pt nanoparticles. *J Inorg Organomet Polym* 2000, 10:145–156.
47. Gu J, Guo Y, Jiang Y-Y, Zhu W, Xu Y-S, Zhao Z-Q, Liu J-X, Li W-X, Jin C-H, Yan C-H, Zhang Y-W. Robust phase control through hetero-seeded epitaxial growth for face-centered cubic Pt@ Ru nanotetrahedrons with superior hydrogen electro-oxidation activity. *J Phys Chem C* 2015, 119:17697–17706.
48. Jin H, Lee KW, Khi NT, An H, Park J, Baik H, Kim J, Yang H, Lee K. Rational synthesis of heterostructured M/Pt (M = Ru or Rh) octahedral nanoboxes and octapods and their structure-dependent electrochemical activity toward the oxygen evolution reaction. *Small* 2015, 11:4462–4468.
49. Lundeen A, Poe R. In: Mc Ketta JJ, Cunningham WA, eds. *Encyclopedia of chemical processing and design*, vol. 2. New York, NY: Marcel Dekker Inc; 1977.
50. Ding YJ, Zhu HJ, Wang, T, Jiao GP, Lu Y. U.S. Patent 7,468,396, 2008.
51. Ding YJ, Zhu HJ, Wang T, Jiao GP, Lu Y. U.S. Patent 7,670,985, 2010
52. Xu X, Scholten J, Mausbeck D. Stability of copper/cobalt catalysts for the synthesis of higher alcohols from syngas. *Applied Catalysis A: General* 1992, 82:91–109.
53. Volkova G, Yurieva T, Plyasova L, Naumova M, Zaikovskii V. Role of the Cu–Co alloy and cobalt carbide in higher alcohol synthesis. *J Mol Catal A: Chem* 2000, 158:389–393.
54. Lebarbier VM, Mei D, Kim DH, Andersen A, Male JL, Holladay JE, Rousseau R, Wang Y. Effects of La_2O_3 on the mixed higher alcohols synthesis from syngas over Co catalysts: a combined theoretical and experimental study. *J Phys Chem C* 2011, 115:17440–17451.
55. Pei Y-P, Liu J-X, Zhao Y-H, Ding Y-J, Liu T, Dong W-D, Zhu H-J, Su H-Y, Yan L, Li J-L, et al. High alcohols synthesis via Fischer–Tropsch reaction at cobalt metal/carbide interface. *ACS Catal* 2015, 5:3620–3624.
56. Levy R, Boudart M. Platinum-like behavior of tungsten carbide in surface catalysis. *Science* 1973, 181:547–549.
57. Saib AM, Moodley DJ, Ciobîcă IM, Hauman MM, Sigwebela BH, Weststrate CJ, Niemantsverdriet JW, van de Loosdrecht J. Fundamental understanding of deactivation and regeneration of cobalt Fischer–Tropsch synthesis catalysts. *Catal Today* 2010, 154:271–282.
58. Dong W, Liu J, Zhu H, Ding Y, Pei Y, Liu J, Du H, Jiang M, Liu T, Su H, et al. Co–Co_2C and Co–Co_2C/AC catalysts for hydroformylation of 1-hexene under low pressure: experimental and theoretical studies. *J Phys Chem C* 2014, 118:19114–19122.
59. de Smit E, Cinquini F, Beale AM, Safonova OV, van Beek W, Sautet P, Weckhuysen BM. Stability and reactivity of ϵ–χ–θ iron carbide catalyst phases in Fischer–Tropsch synthesis: controlling μC. *J Am Chem Soc* 2010, 132:14928–14941.
60. Niemantsverdriet JW, Vanderkraan AM, Vandijk WL, Vanderbaan HS. Behavior of metallic iron catalysts during Fischer-Tropsch synthesis studied with Mossbauer-spectroscopy, X-ray-diffraction, carbon content determination, and reaction kinetic measurements. *J Phys Chem* 1980, 84:3363–3370.
61. Kuei CK, Lee MD. Temperature-programmed reaction of preadsorbed Co on iron catalyst – new experimental-evidence for competition model. *J Mol Catal* 1991, 65:293–305.
62. Amelse JA, Butt JB, Schwartz LH. Carburization of supported iron synthesis catalysts. *J Phys Chem* 1978, 82:558–563.
63. Bukur DB, Nowicki L, Manne RK, Lang XS. Activation studies with a precipitated iron catalyst for fischer-tropsch synthesis. 2. Reaction studies. *J Catal* 1995, 155:366–375.
64. Bukur DB, Okabe K, Rosynek MP, Li CP, Wang DJ, Rao KRPM, Huffman GP. Activation studies with a precipitated iron catalyst for Fischer-Tropsch synthesis. 1. Characterization studies. *J Catal* 1995, 155:353–365.

 © 2016 John Wiley & Sons, Ltd

65. Badani MV, Delgass WN. The active phase of iron catalysts for acetonitrile synthesis. *J Catal* 1999, 187:506–517.
66. Mansker LD, Jin YM, Bukur DB, Datye AK. Characterization of slurry phase iron catalysts for Fischer-Tropsch synthesis. *Appl Catal A: Gen* 1999, 186:277–296.
67. Rao KRPM, Huggins FE, Ganguly B, Mahajan V, Huffman GP, Davis B, Obrien RJ, Xu LG, Rao VUS. Effect of pre-heat treatment on a Fischer-Tropsch iron catalyst. *Hyperfine Interact* 1994, 93:1755–1758.
68. Schulz H, Riedel T, Schaub G. Fischer-Tropsch principles of co-hydrogenation on iron catalysts. *Top Catal* 2005, 32:117–124.
69. Herranz T, Rojas S, Perez-Alonso FJ, Ojeda M, Terreros P, Fierro JLG. Genesis of iron carbides and their role in the synthesis of hydrocarbons from synthesis gas. *J Catal* 2006, 243:199–211.
70. Hao QL, Bai L, Xiang HW, Li YW. Phase transformations of a spray-dried iron catalyst for slurry Fischer-Tropsch synthesis during activation and reaction. *Fuel Process Technol* 2008, 89:1358–1364.
71. Zhao H, Liu J-X, Yang C, Yao S, Su H-Y, Dong M, Wang J, Hou Y, Li W-X, Ma D. Phase dependence of iron catalysts for Fischer-Tropsch synthesis: metal versus carbide. *Energy Environ Sci*. In press.
72. Wang T, Tian X-X, Li Y-W, Wang J, Beller M, Jiao H. Coverage-dependent CO adsorption and dissociation mechanisms on iron surfaces from DFT computations. *ACS Catal* 2014, 4:1991–2005.
73. Sorescu DC. Plane-wave density functional theory investigations of the adsorption and activation of CO on Fe_5C_2 surfaces. *J Phys Chem C* 2009, 113:9256–9274.
74. Zhao S, Liu X-W, Huo C-F, Li Y-W, Wang J, Jiao H. Determining surface structure and stability of ε-Fe_2C, χ-Fe_5C_2, θ-Fe_3C and Fe_4C phases under carburization environment from combined DFT and atomistic thermodynamic studies. *Catal Struct React* 2015, 1:44–60.
75. Liang S, Teng F, Bulgan G, Zong R, Zhu Y. Effect of phase structure of MnO_2 nanorod catalyst on the activity for CO oxidation. *J Phys Chem C* 2008, 112:5307–5315.
76. He D, Ding Y, Luo H, Li C. Effects of zirconia phase on the synthesis of higher alcohols over zirconia and modified zirconia. *J Mol Catal A: Chem* 2004, 208:267–271.
77. Muscat J, Swamy V, Harrison NM. First-principles calculations of the phase stability of TiO_2. *Phys Rev B* 2002, 65:224112.
78. Zhu J, Zheng W, He B, Zhang J, Anpo M. Characterization of Fe–TiO_2 photocatalysts synthesized by hydrothermal method and their photocatalytic reactivity for photodegradation of XRG dye diluted in water. *J Mol Catal A: Chem* 2004, 216:35–43.
79. Karakitsou KE, Verykios XE. Effects of altervalent cation doping of titania on its performance as a photocatalyst for water cleavage. *J Phys Chem* 1993, 97:1184–1189.
80. Ohno T, Sarukawa K, Tokieda K, Matsumura M. Morphology of a TiO_2 photocatalyst (Degussa, P-25) consisting of anatase and rutile crystalline phases. *J Catal* 2001, 203:82–86.
81. Bickley RI, Gonzalez-Carreno T, Lees JS, Palmisano L, Tilley RJ. A structural investigation of titanium dioxide photocatalysts. *J Solid State Chem* 1991, 92:178–190.
82. Zhang J, Xu Q, Feng Z, Li M, Li C. Importance of the relationship between surface phases and photocatalytic activity of TiO_2. *Angew Chem Int Ed* 2008, 47:1766–1769.
83. Zhao W-N, Liu Z-P. Mechanism and active site of photocatalytic water splitting on titania in aqueous surroundings. *Chem Sci* 2014, 5:2256–2264.

 © 2016 John Wiley & Sons, Ltd